Segmentation of a vector field: Dominant parameter and shape optimization

Tristan Roy, Eric Debreuve, Michel Barlaud, Gilles Aubert

Segmentation of a vector field: Dominant parameter and shape optimization

Tristan Roy[†] Éric Debreuve[†] Michel Barlaud[†] Gilles Aubert[‡]

PREPRINT – Published in *Journal of Mathematical Imaging and Vision*

Abstract

Vector field segmentation methods usually belong to either of three classes: methods which segment regions homogeneous in direction and/or norm, methods which detect discontinuities in the vector field, and region growing or classification methods. The first two classes of method do not allow segmentation of complex vector fields and control of the type of fields to be segmented, respectively. The third class does not directly allow a smooth representation of the segmentation boundaries. In the particular case where the vector field actually represents an optical flow, a fourth class of methods acts as a detector of main motion. The proposed method combines a vector field model and a theoretically founded minimization approach. Compared to existing methods following the same philosophy, it relies on an intuitive, geometric way to define the model while preserving a general point of view adapted to the segmentation of potentially complex vector fields with the condition that they can be described by a finite number of parameters. The energy to be minimized is deduced from the choice of a specific class of field lines, *e.g.* straight lines or circles, described by the general form of their parametric equations. In that sense, the proposed method is a principled approach for segmenting parametric vector fields. The minimization problem was rewritten into a shape optimization and implemented by spline-based active contours. The algorithm was applied to the segmentation of precomputed optical flow fields given by an external, independent algorithm.

Keywords: Segmentation, vector field, dominant parameter, shape optimization, optical flow

[†]Laboratoire I3S, UMR CNRS 6070, Les Algorithmes, Bât. Euclide B, 2000, route des lucioles, BP 121, 06903 Sophia Antipolis Cedex, France (triroy@math.ucla.edu - barlaud,debreuve@i3s.unice.fr).

[‡]Laboratoire Dieudonné, UMR CNRS 6621, Université de Nice-Sophia Antipolis, Parc Valrose, 06108 Nice Cedex 2, France (gaubert@math.unice.fr).

1 Introduction

A segmentation of a vector field is a partition of the domain of the field into subdomains such that each subdomain is as homogeneous as possible in terms of a certain homogeneity function. The standard deviation of the directions of the vectors contained in a subdomain is an example of a homogeneity function. The function may or may not be the same for each subdomain.

Segmentation of vector fields is part of a wider class of problems that can be called multichannel segmentation. Segmentation of color images is an example of such problems [26, 29]. More generally, it corresponds to the segmentation of an n-vector valued function. It can be solved by extending a single-channel method [23] by substituting a vectorial similarity measure, *e.g.* a weighted sum of the individual component similarities [28], for the scalar similarity measure. However, this straightforward extension does not allow to describe complex region characteristics. Basically, as far as vector fields are concerned, regions homogeneous in direction and/or norm can be detected. The dual approach is to detect discontinuities in the vector field [15]. However, this approach is usually not suitable to determine regions necessary for subsequent processing tasks and it does not allow to control the type of fields to be segmented. Using the terminology of optical flow, the main motion can be segmented by thresholding the vector field magnitude [11] or, similarly, the image of frame-to-frame difference [34] of a video sequence. Even if the region of main motion is found based on a motion model [34], this kind of methods are better described as motion detections than motion segmentations. In order to segment complex vector fields or motions, the use of a model seems appropriate. A region growing, or merging, technique can be used to iteratively group pixels or patches together when they respect a common motion model (or vector field model). Precision can be increased while preserving coherence by implementing successive steps with increasing model complexity [9]. However, a threshold is necessary in order to determine when to stop merg-

ing. This can be avoided by replacing the merging decision with a classification algorithm [32]. Indeed, classification relates to a notion of closest distance with respect to motion candidates. Unfortunatelty, such a method is strongly constrained by the discretization of the vector field domain (pixels or patches). It might be difficult to impose only some smoothness to the segmentation boundary. A minimization approach with respect to the segmentation domains also allows to get rid of the thresholding while giving more flexibility to the representation of the domains [30, 12, 27, 13]. These methods are adapted to optical flow segmentation (explicitly or implicitly when the input is a video sequence [12, 13]) and might not be intuitive enough when it comes to segment a vector field not directly related to a motion.

The proposed method follows the same philosophy combining a model and a theoretically founded minimization approach. Compared to existing methods, it relies on an intuitive, geometric way to define the model while preserving a general point of view adapted to the segmentation of potentially complex vector fields of $\mathbb{R}^2$ with the condition that they can be described by a finite number of parameters.

2 Proposed approach

2.1 Context

The vector field to be segmented is denoted by E. Its components are denoted by E_1 and E_2. The field is assumed to be smooth and normalized (the norm of E is equal to one everywhere). Two examples of vector fields are shown in Fig. 1.

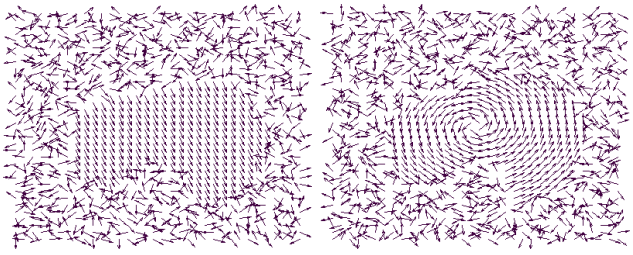

Figure 1: Two examples of vector fields: translation *(left)* and rotation *(right)*.

We recall that L is a field line of E if and only if

$$\dot{x}_1(p)\ E_2(x(p)) - \dot{x}_2(p)\ E_1(x(p)) = 0 \qquad (1)$$

and

$$\dot{x}(p) \neq 0 \qquad (2)$$

where $x(p)$ is the equation of L, p belongs to a certain interval $[a, b]$, and $\dot{x}$ represents the derivative of x with respect to p. Equation (1) represents the fact that the vector field is orthogonal to the normal along any field line (or, equivalently, collinear to the tangent) and Eq. (2) represents the fact that the norm of the tangent is never equal to zero.

A typical example of vector fields in video is optical flow [22, 18, 30, 5, 3, 33], *i.e.*, the vector field describing the apparent motion between two successive frames of a video sequence. In this context, if W is the optical flow between frames f_t and f_{t+1}, then E is given by

$$\begin{cases} E = \dfrac{W}{|W|} \\ f_{t+1}(x + W(x)) = f_t(x) \end{cases} . \qquad (3)$$

We will use the segmentation of precomputed optical flow fields as an illustration of the proposed method. We will assume that the optical flows are given by an external, independent algorithm.

2.2 Variational formulation

A segmentation problem can be solved in a variational context by defining an energy to be minimized. This energy is obviously a function of the boundaries of some/all of the segmentation domains (contour-based segmentation) and/or their regions (region-based segmentation). For simplicity, we will only consider the case of two domains: the object and the background. The term "object" must be understood as a region with specific characteristics and the expression "object domain" must be understood as an estimation of the actual region of the object. In the case of region-based segmentation, if both the object and the background domains are taken into account, the segmentation is said to involve region competition. When only the object domain is used, the energy is classically an integral on the object domain of a function characterizing the object that should be detected. This function is non-negative and it is ideally equal to zero on the region of the object. It relates to a notion of homogeneity of the object in a broad sense. Our purpose is to find such functions and to provide a general method for the segmentation of vector fields of $\mathbb{R}^2$ that can be described by a finite number of parameters. These functions are deduced from the choice of a specific class of field lines, *e.g.* straight lines or circles, described by the general form of their parametric equations.

The general form of the proposed energies is

$$J(\Omega) = \int_\Omega h(E, \Omega, x)\ \mathrm{d}x \qquad (4)$$

where E is the vector field to be segmented and Ω is the unknown segmentation domain. Minimization of this type of energy requires special care since the set $\mathcal{F}$ of domains included in the image region, a bounded, connected, open set of $\mathbb{R}^2$, is not a vectorial space. The

shape gradient approach is adapted to this problem. Although this aspect is not an original contribution of the paper, we will present it briefly in Section 2.3 since it is a prerequisite to the understanding of the actual contributions presented in Sections 3, 4, and 5.

2.3 Shape derivative

The shape derivative is a measure of the influence of a deformation of Ω on the value of (4). It is a function of Ω and of the deformation, V, a function from $\mathbb{R}$ to $\mathbb{R}^2$. In order to be derived, energy (4) should first be rewritten as a function of a deformation parameter τ

$$J(\tau) = \int_{\Omega(\tau)} h(E, \tau, x) \, \mathrm{d}x \; . \tag{5}$$

By definition, parameter τ is such that

$$\Omega(\tau) = T_\tau(\Omega(\tau = 0)) \tag{6}$$

where $\Omega(\tau = 0)$ is an initial domain and T_τ is an unknown transformation that must be such that

$$\lim_{\tau \to \infty} \Omega(\tau) = \hat{\Omega} \tag{7}$$

where $\hat{\Omega}$ is the unique global minimizer of (4) (if this minimizer exists). Then, it was shown that [14, 2, 17, 20]

$$\frac{\mathrm{d}J}{\mathrm{d}\tau}(\tau, V) = \int_{\Omega(\tau)} \frac{\partial h}{\partial \tau}(E, \tau, x) \, \mathrm{d}x - \int_{\partial\Omega(\tau)} h(E, \tau, x(s)) \; V(s) \; N_\tau(s) \, \mathrm{d}s \tag{8}$$

where $\partial\Omega(\tau)$ is the oriented boundary of $\Omega(\tau)$, s is the arclength along $\Omega(\tau)$, and N_τ is the inward unit normal of $\Omega(\tau)$. Given a domain $\Omega(\tau)$, we would like to know which deformation should be applied to $\Omega(\tau)$ in order to obtain a new domain "closer" to the domain for which (5) is minimal, if this domain exists and is unique. However, the first integral of (8) does not involve V explicitly. In other words, it is not readily usable. Nevertheless, function h is assumed to be such that there exists a function $\tilde{h}$ such that

$$\int_{\Omega(\tau)} \frac{\partial h}{\partial \tau}(E, \tau, x) \, \mathrm{d}x = \int_{\partial\Omega(\tau)} \tilde{h}(E, \tau, x(s)) \; V(s) \; N_\tau(s) \, \mathrm{d}s \; . \tag{9}$$

Actually, in some circumstances, this integral is equal to zero. It will be the case for the energies proposed in Sections 3, 4, and 5. Therefore, Section 2.4 is written for this case only.

2.4 Minimization algorithm

Since the purpose is to minimize (5), deformation V must be chosen such that derivative (8) is negative. As noted in Section 2.3, the first integral of (8) will be equal to zero in our case. Clearly, the following expression satisfies this condition

$$V_\tau = h(E, \tau, x) \; N_\tau \; . \tag{10}$$

Applying successive deformations (10) to $\Omega(\tau)$ for increasing values of τ, domain Ω (seen as a function of τ) should converge toward the unique global minimizer of (4) (if this minimizer exists). This is typically an active contour process [21, 7, 26, 8] whose evolution equation is, noting that V_τ is equal to $\frac{\partial \Gamma}{\partial \tau}$ where Γ is a short notation for $\partial\Omega$,

$$\begin{cases} \dfrac{\partial \Gamma}{\partial \tau}(\tau) = h(E, \tau, x) \; N_\tau \\ \Gamma(\tau = 0) = \Gamma_0 \end{cases} \tag{11}$$

where Γ_0 is an initial guess, or estimate, of the segmentation contour. Therefore, the minimization of (4) can be achieved by iteratively deforming a contour according to (11) until (8) is equal to zero.

3 Segmentation of translation domains

3.1 Translation domain

Let $\mathcal{C}$ be the unit circle of $\mathbb{R}^2$ and let $\mathcal{C}^+$ be the subset of $\mathcal{C}$ defined by $(cos(\theta), sin(\theta))$, $\theta \in]-\pi/2, \pi/2]$.

A region of the domain of E containing only field lines that are straight lines is called a translation domain (See Fig. 1). Equivalently, a domain Ω of $\mathcal{F}$ is a translation domain if and only if there exists a unique parameter $a(\Omega)$ of $\mathcal{C}^+$ such that for any field line L verifying $L \cap \Omega \neq \emptyset$ there exists a unique constant $c(L)$ of $\mathbb{R}$ such that

$$a(\Omega) \cdot x = c(L), \;\; x \in L \cap \Omega \; . \tag{12}$$

Vector $a(\Omega)$ is called the translation parameter of Ω. It is actually the normal to the straight field lines. In our context, the specific value of $c(L)$ is of no importance and plays the role of an unnecessary parameter. Therefore, a condition equivalent to (12) while not involving $c(L)$ should be found. Let us parametrize L by p. For any $x(p)$ of $L \cap \Omega$

$$a(\Omega) \cdot x(p) = c(L) \tag{13}$$

$$\iff a_1(\Omega) x_1(p) + a_2(\Omega) x_2(p) = c(L) \; . \tag{14}$$

The derivative of (14) with respect to p combined with (1) leads to the following system of equations

$$\begin{pmatrix} a_1(\Omega) & a_2(\Omega) \\ E_2(x(p)) & -E_1(x(p)) \end{pmatrix} \dot{x}(p) = M \; \dot{x}(p) = 0 \; . \tag{15}$$

Combining (2) and (15), it can be concluded that the determinant of M must be equal to zero. Therefore, a domain Ω of $\mathcal{F}$ is a translation domain if and only if there exists a unique $a(\Omega)$ of $\mathcal{C}^+$ such that for any x of Ω

$$a(\Omega) \cdot E(x) = 0 \ . \tag{16}$$

3.2 Dominant translation parameter

From (16), it can be deduced that if Ω is a translation domain then $a(\Omega)$ is a global minimizer of

$$\begin{aligned} K_\Omega^{\text{tra}} : \mathcal{C}^+ &\to \mathbb{R} \\ \alpha &\mapsto \int_\Omega (\alpha \cdot E(x))^2 \ \mathrm{d}x \ . \end{aligned} \tag{17}$$

Indeed, K_Ω^{tra} is clearly nonnegative and $K_\Omega^{\text{tra}}(a(\Omega))$ is equal to zero. Moreover, this minimizer is unique in $\mathcal{C}^+$ since any candidate must satisfy (16), *i.e.*, must be orthogonal to E. Therefore, it must be collinear to $a(\Omega)$, *i.e.*, equal to $a(\Omega)$ in $\mathcal{C}^+$.

Looking from a domain point of view (as opposed to the parameter point of view), it can also be deduced from (16) that Ω minimizes the following energy

$$\begin{aligned} G^{\text{tra}} : \mathcal{F} &\to \mathbb{R} \\ \omega &\mapsto \int_\omega (a(\omega) \cdot E(x))^2 \ \mathrm{d}x \end{aligned} \tag{18}$$

with $a(\omega)$ defined as the unique global minimizer of K_ω^{tra}.

However, there is no guarantee that for any ω of $\mathcal{F}$ there exists a unique global minimizer of K_ω^{tra} and that K_ω^{tra} is equal to zero for this minimizer. In other words, ω might not have a translation parameter (namely, if it is not a translation domain). Nevertheless, as long as K_ω^{tra} has a unique global minimizer $\hat{a}(\omega)$, this minimizer is called the dominant translation parameter of ω.

3.3 Practical formulation

It is clear that any subdomain of a translation domain is a minimizer of energy (18). As a consequence, the problem of finding translation domains should be reformulated in finding translation domains having an area as big as possible. This is equivalent to minimizing $G^{\text{tra}}(\Omega)$ while maximizing the area of Ω, *i.e.*, minimizing the following energy

$$\begin{aligned} J^{\text{tra}} : \mathcal{F}^{\text{tra}} &\to \mathbb{R} \\ \Omega &\mapsto \int_\Omega (\hat{a}(\Omega) \cdot E(x))^2 \ \mathrm{d}x - \mu \int_\Omega \mathrm{d}x \end{aligned} \tag{19}$$

where $\mathcal{F}^{\text{tra}}$ is the set of domains of $\mathcal{F}$ having a dominant translation parameter, $\hat{a}(\Omega)$ is the dominant translation parameter of Ω, and μ is a positive constant.

Certainly, the minimization algorithm will require computation of $\hat{a}(\Omega)$. However, this latter aspect will be presented later in Section 3.5 when it will be clear where exactly this parameter is needed in the overall process.

3.4 Shape derivative

Following the methodology of Section 2.3, energy (19) is rewritten as a function of an evolution parameter τ

$$J^{\text{tra}}(\tau) = \int_{\Omega(\tau)} (\hat{a}(\tau) \cdot E(x))^2 \ \mathrm{d}x - \mu \int_{\Omega(\tau)} \mathrm{d}x \tag{20}$$

where $\hat{a}(\tau)$ is a short notation for $\hat{a}(\Omega(\tau))$. Applying result (8) to each integral, the shape derivative of (20) can be computed

$$\begin{aligned} \frac{\mathrm{d}J^{\text{tra}}}{\mathrm{d}\tau}(\tau, V) = &\int_{\Omega(\tau)} \frac{\mathrm{d}}{\mathrm{d}\tau} (\hat{a}(\tau) \cdot E(x))^2 \ \mathrm{d}x \\ &- \int_{\partial\Omega(\tau)} (\hat{a}(\tau) \cdot E(s))^2 \ V(s) \cdot N_\tau(s) \ \mathrm{d}s \\ &- \int_{\Omega(\tau)} \frac{\mathrm{d}\mu}{\mathrm{d}\tau} \ \mathrm{d}x \\ &+ \int_{\partial\Omega(\tau)} \mu \ V(s) \cdot N_\tau(s) \ \mathrm{d}s \end{aligned} \tag{21}$$

$$\begin{aligned} = &\frac{\mathrm{d}\hat{a}}{\mathrm{d}\tau}(\tau) \int_{\Omega(\tau)} \frac{\mathrm{d}}{\mathrm{d}\alpha} (\alpha \cdot E(x))^2 |_{\hat{a}(\tau)} \ \mathrm{d}x \\ &- \int_{\partial\Omega(\tau)} (\hat{a}(\tau) \cdot E(s))^2 \ V(s) \cdot N_\tau(s) \ \mathrm{d}s \\ &+ \int_{\partial\Omega(\tau)} \mu \ V(s) \cdot N_\tau(s) \ \mathrm{d}s \end{aligned} \tag{22}$$

$$\begin{aligned} = &\frac{\mathrm{d}\hat{a}}{\mathrm{d}\tau}(\tau) \ \frac{\mathrm{d}}{\mathrm{d}\alpha} \left(\int_{\Omega(\tau)} (\alpha \cdot E(x))^2 \ \mathrm{d}x \right) |_{\hat{a}(\tau)} \\ &- \int_{\partial\Omega(\tau)} \left[(\hat{a}(\tau) \cdot E(s))^2 - \mu \right] \ V(s) \cdot N_\tau(s) \ \mathrm{d}s \end{aligned} \tag{23}$$

$$\begin{aligned} = &\frac{\mathrm{d}\hat{a}}{\mathrm{d}\tau}(\tau) \ \frac{\mathrm{d}K_{\Omega(\tau)}^{\text{tra}}}{\mathrm{d}\alpha} |_{\hat{a}(\tau)} \\ &- \int_{\partial\Omega(\tau)} \left[(\hat{a}(\tau) \cdot E(s))^2 - \mu \right] \ V(s) \cdot N_\tau(s) \ \mathrm{d}s \end{aligned} \tag{24}$$

where $E(s)$ is a short notation for $E(x(s))$. Expression (24) still contains a surface integral. As explained in Section 2.3, the shape derivative is readily usable if it contains only a line integral. Parameter $\hat{a}(\tau)$ minimizes $K_{\Omega(\tau)}^{\text{tra}}$ on $\mathcal{C}^+$. However, since $K_{\Omega(\tau)}^{\text{tra}}$ is an even function, $\hat{a}(\tau)$ also minimizes it on $\mathcal{C}$. Vectors of $\mathcal{C}$ respect the following constraint

$$\phi(\alpha) = |\alpha|^2 - 1 = 0 \ . \tag{25}$$

Therefore, there exists a Lagrange multiplier λ_τ such that

$$\frac{\mathrm{d}K^{\mathrm{tra}}_{\Omega(\tau)}}{\mathrm{d}\alpha}|_{\hat{a}(\tau)} = \lambda_\tau \ \frac{\mathrm{d}\phi}{\mathrm{d}\alpha}|_{\hat{a}(\tau)} \ . \tag{26}$$

Using (26) in (24), the shape derivative of (20) is

$$\begin{aligned}\frac{\mathrm{d}J^{\mathrm{tra}}}{\mathrm{d}\tau}(\tau, V) &= \lambda_\tau \ \frac{\mathrm{d}\hat{a}}{\mathrm{d}\tau}(\tau) \ \frac{\mathrm{d}\phi}{\mathrm{d}\alpha}|_{\hat{a}(\tau)} \\ &\quad - \int_{\partial\Omega(\tau)} \left[(\hat{a}(\tau)\cdot E(s))^2 - \mu\right] \ V(s)\cdot N_\tau(s) \ \mathrm{d}s \end{aligned} \tag{27}$$

$$\begin{aligned}&= \lambda_\tau \ \frac{\mathrm{d}}{\mathrm{d}\tau}\phi(\hat{a}(\tau)) \\ &\quad - \int_{\partial\Omega(\tau)} \left[(\hat{a}(\tau)\cdot E(s))^2 - \mu\right] \ V(s)\cdot N_\tau(s) \ \mathrm{d}s\end{aligned} \tag{28}$$

Since $\phi(\hat{a}(\tau))$ is constant with respect to τ, the final expression of the shape derivative of (20) is

$$\frac{\mathrm{d}J^{\mathrm{tra}}}{\mathrm{d}\tau}(\tau, V) = -\int_{\partial\Omega(\tau)} \left[(\hat{a}(\tau)\cdot E(s))^2 - \mu\right] \ V(s)\cdot N_\tau(s) \ \mathrm{d}s \ . \tag{29}$$

3.5 Minimization algorithm

As presented in Section 2.3, the minimization of (19) can be achieved by iterating an active contour evolution equation deduced from shape derivative (29). The evolution equation is

$$\frac{\partial\Gamma}{\partial\tau}(\tau) = \left[(\hat{a}(\tau)\cdot E)^2 - \mu\right] \ N_\tau \tag{30}$$

where $\Gamma(\tau = 0)$ is an initial estimate of the segmentation contour. Dominant translation parameter $\hat{a}(\tau)$ of $\Omega(\tau)$ must be computed in order to implement evolution (30). In Section 3.2, $\hat{a}(\tau)$ was expressed as the unique global minimizer of $K^{\mathrm{tra}}_{\Omega(\tau)}$. Although expression (17) is not readily usable, it can be rewritten as follows

$$K^{\mathrm{tra}}_{\Omega(\tau)}(\alpha) = \alpha^T \left(\int_{\Omega(\tau)} E(x) \ E(x)^T \ \mathrm{d}x\right) \alpha \tag{31}$$

$$= \alpha^T \ Q_\tau \ \alpha \ . \tag{32}$$

Matrix Q_τ is clearly symmetric and real. Therefore, it has real eigenvalues δ_1 and δ_2. Without loss of generality, it is assumed that $\delta_1 \leq \delta_2$. Rewritting (32) in an orthonormal basis of eigenvectors, we have

$$K^{\mathrm{tra}}_{\Omega(\tau)}(\alpha) = \delta_1 \ \alpha_1^2 + \delta_2 \ \alpha_2^2 \tag{33}$$

$$= (\delta_1 - \delta_2) \ \alpha_1^2 + \delta_2 \tag{34}$$

since we look for α in $\mathcal{C}^+$ ($\alpha_1^2 + \alpha_2^2 = 1$). If δ_1 and δ_2 are equal, $K^{\mathrm{tra}}_{\Omega(\tau)}$ is constant on $\mathcal{C}^+$. Therefore, a necessary and sufficient condition of uniqueness of $\hat{a}(\tau)$ is that Q_τ has two distinct eigenvalues. In other words, Q_τ must not be equal to the identity matrix times a constant. In this case, $K^{\mathrm{tra}}_{\Omega(\tau)}$ is minimum when α_1 is equal to one, which implies that α_2 is equal to zero. Since α has been expressed in a basis of eigenvectors, it is actually equal to the eigenvector of $\mathcal{C}^+$ associated with eigenvalue δ_1. In brief, $\hat{a}(\tau)$ is the unique solution in $\mathcal{C}^+$ of

$$Q_\tau \ \alpha = \delta_{\min} \ \alpha \tag{35}$$

where $\delta_{\min}$ is the lowest eigenvalue of Q_τ.

In Appendix A, we propose a sufficient condition of nonexistence of a dominant translation parameter as an illustration of the case where Q_τ is equal to the identity matrix times a constant.

Given the proposed iterative method, there is a concern about the choice of an initial contour $\Gamma(\tau = 0)$. Indeed, it must be such that $\Omega(\tau = 0)$ is a domain of $\mathcal{F}^{\mathrm{tra}}$. Furthermore, this property should hold for all τ positive, until convergence. As explained in Appendix C, a sufficient condition is that $\Omega(\tau = 0)$ contains domain Ω^{tra}, minimizer of (19), entirely while not exceeding an area of $1 + \frac{\sqrt{2}}{2}$ times the area of Ω^{tra}. Naturally, since Ω^{tra} is unknown, it implies the impossibility of a "blind" initialization. Nevertheless, it is not uncommon to have such constraints in the field of segmentation using active contours.

4 Segmentation of rotation domains

4.1 Rotation domain

A region of the domain of E containing only field lines that are circles is called a rotation domain (See Fig. 1). Equivalently, a domain Ω of $\mathcal{F}$ is a rotation domain if and only if there exists a unique parameter $a(\Omega)$ of $\mathbb{R}^2$ such that for any field line L verifying $L \cap \Omega \neq \emptyset$ there exists a unique constant $c(L)$ of $\mathbb{R}$ such that

$$|x - a(\Omega)|^2 = c(L), \ x \in L \cap \Omega \ . \tag{36}$$

Vector $a(\Omega)$ is called the rotation parameter of Ω. It is actually the center of the circular field lines. In our context, the specific value of $c(L)$ is of no importance and plays the role of an unnecessary parameter. Therefore, a condition equivalent to (36) while not involving $c(L)$ should be found. Let us parametrize L by p. For any $x(p)$ of $L \cap \Omega$

$$|x(p) - a(\Omega)|^2 = c(L) \tag{37}$$

$$\iff (x_1(p) - a_1)^2 + (x_2(p) - a_2)^2 = c(L) \tag{38}$$

The derivative of (38) with respect to p combined with (1) leads to the following system of equations

$$\begin{pmatrix} x_1(p) - a_1 & x_2(p) - a_2 \\ E_2(x(p)) & -E_1(x(p)) \end{pmatrix} \dot{x}(p) = M\ \dot{x}(p) = 0\ . \tag{39}$$

Combining (2) and (39), it can be concluded that the determinant of M must be equal to zero. Therefore, a domain Ω of $\mathcal{F}$ is a rotation domain if and only if there exists a unique $a(\Omega)$ of $\mathbb{R}^2$ such that for any x of Ω

$$(x - a(\Omega)) \cdot E(x) = 0\ . \tag{40}$$

4.2 Dominant rotation parameter

From (40), it can be deduced that if Ω is a rotation domain then $a(\Omega)$ is a global minimizer of

$$\begin{aligned} K_\Omega^{\text{rot}} : \mathbb{R}^2 &\to \mathbb{R} \\ \alpha &\mapsto \int_\Omega ((x - \alpha) \cdot E(x))^2\ \mathrm{d}x\ . \end{aligned} \tag{41}$$

Indeed, K_Ω^{rot} is clearly nonnegative and $K_\Omega^{\text{rot}}(a(\Omega))$ is equal to zero. Moreover, this minimizer is unique in $\mathbb{R}^2$ (See Section 4.5).

Looking from a domain point of view (as opposed to the parameter point of view), it can also be deduced from (40) that Ω minimizes the following energy

$$\begin{aligned} G^{\text{rot}} : \mathcal{F} &\to \mathbb{R} \\ \omega &\mapsto \int_\omega ((x - a(\omega)) \cdot E(x))^2\ \mathrm{d}x \end{aligned} \tag{42}$$

with $a(\omega)$ defined as the unique global minimizer of K_ω^{rot}.

However, there is no guarantee that for any ω of $\mathcal{F}$ there exists a unique global minimizer of K_ω^{rot} and that K_ω^{rot} is equal to zero for this minimizer. In other words, ω might not have a rotation parameter (namely, if it is not a rotation domain). Nevertheless, as long as K_ω^{rot} has a unique global minimizer $\hat{a}(\omega)$, this minimizer is called the dominant rotation parameter of ω.

4.3 Practical formulation

It is clear that any subdomain of a rotation domain is a minimizer of energy (42). As a consequence, the problem of finding rotation domains should be reformulated in finding rotation domains having an area as big as possible. This is equivalent to minimizing $G^{\text{rot}}(\Omega)$ while maximizing the area of Ω, *i.e.*, minimizing the following energy

$$\begin{aligned} J^{\text{rot}} : \mathcal{F}^{\text{rot}} &\to \mathbb{R} \\ \Omega &\mapsto \int_\Omega ((x - \hat{a}(\Omega)) \cdot E(x))^2\ \mathrm{d}x - \mu \int_\Omega \mathrm{d}x \end{aligned} \tag{43}$$

where $\mathcal{F}^{\text{rot}}$ is the set of domains of $\mathcal{F}$ having a dominant rotation parameter, $\hat{a}(\Omega)$ is the dominant rotation parameter of Ω, and μ is a positive constant.

Certainly, the minimization algorithm will require computation of $\hat{a}(\Omega)$. However, this latter aspect will be presented later in Section 4.5 when it will be clear where exactly this parameter is needed in the overall process.

4.4 Shape derivative

Following the methodology of Section 2.3, energy (43) is rewritten as a function of an evolution parameter τ

$$J^{\text{rot}}(\tau) = \int_{\Omega(\tau)} ((x - \hat{a}(\tau)) \cdot E(x))^2\ \mathrm{d}x - \mu \int_{\Omega(\tau)} \mathrm{d}x \tag{44}$$

where $\hat{a}(\tau)$ is a short notation for $\hat{a}(\Omega(\tau))$. Applying result (8) to each integral, the shape derivative of (44) can be computed in a way similar to the development presented in Section 3.4. The only difference is that, in the rotation case, parameter $\hat{a}(\tau)$ minimizes $K_{\Omega(\tau)}^{\text{rot}}$ on $\mathbb{R}^2$. In other words, there are no constraints on $\hat{a}(\tau)$. As a consequence, it can be concluded that $\mathrm{d}K_{\Omega(\tau)}^{\text{rot}}/\mathrm{d}\alpha|_{\hat{a}(\tau)}$ is equal to zero without involving a Lagrange multiplier. The shape derivative of (44) is

$$\begin{aligned} \frac{\mathrm{d}J^{\text{rot}}}{\mathrm{d}\tau}(\tau, V) = -\int_{\partial\Omega(\tau)} &\left[((x(s) - \hat{a}(\tau)) \cdot E(s))^2 - \mu\right] \\ &V(s) \cdot N_\tau(s)\ \mathrm{d}s\ . \end{aligned} \tag{45}$$

4.5 Minimization algorithm

As presented in Section 2.3, the minimization of (43) can be achieved by iterating an active contour evolution equation deduced from shape derivative (45). The evolution equation is

$$\frac{\partial \Gamma}{\partial \tau}(\tau) = \left[((x - \hat{a}(\tau)) \cdot E)^2 - \mu\right]\ N_\tau \tag{46}$$

where $\Gamma(\tau = 0)$ is an initial estimate of the segmentation contour. Dominant rotation parameter $\hat{a}(\tau)$ of $\Omega(\tau)$ must be computed in order to implement evolution (46). In Section 4.2, $\hat{a}(\tau)$ was expressed as the unique global minimizer of $K_{\Omega(\tau)}^{\text{rot}}$.

It can easily be shown that

$$H_{K_{\Omega(\tau)}^{\text{rot}}} = 2\ Q_\tau \tag{47}$$

where $H_{K_{\Omega(\tau)}^{\text{rot}}}$ is the Hessian matrix of $K_{\Omega(\tau)}^{\text{rot}}$ and Q_τ is the matrix in (32). Considering (17) and (32), it is clear that Q_τ is nonnegative. As a consequence, $K_{\Omega(\tau)}^{\text{rot}}$ is convex. However, its strict convexity cannot be inferred yet.

If $\hat{a}(\tau)$ actually exists, it is such that

$$\frac{\mathrm{d}K^{\mathrm{rot}}_{\Omega(\tau)}}{\mathrm{d}\alpha}|_{\hat{a}(\tau)}= 0 \tag{48}$$

Although expression (48) is not readily usable, it can be rewritten as follows

$$Q_\tau\ \hat{a}(\tau) = \int_{\Omega(\tau)} (x \cdot E(x))\ E(x)\mathrm{d}x\ . \tag{49}$$

Therefore, a necessary and sufficient condition of existence and uniqueness of $\hat{a}(\tau)$ is that the determinant of Q_τ is not equal to zero. In this case, $\hat{a}(\tau)$ is the unique solution in $\mathbb{R}^2$ of (49), namely

$$\hat{a}(\tau) = Q_\tau^{-1}\ \int_{\Omega(\tau)} (x \cdot E(x))\ E(x)\mathrm{d}x\ . \tag{50}$$

The uniqueness of the solution of (48) implies the strict convexity of $K^{\mathrm{rot}}_{\Omega(\tau)}$. Therefore, it can be concluded that $\hat{a}(\tau)$ is indeed the unique global minimizer of $K^{\mathrm{rot}}_{\Omega(\tau)}$.

In Appendix B, we propose a necessary and sufficient condition of nonexistence of a dominant rotation parameter as an illustration of the case where the determinant Q_τ is equal to zero.

Given the proposed iterative method, there is a concern about the choice of an initial contour $\Gamma(\tau = 0)$. Indeed, it must be such that $\Omega(\tau = 0)$ is a domain of $\mathcal{F}^{\mathrm{rot}}$. Furthermore, this property should hold for all τ positive, until convergence. As explained in Appendix D, a sufficient condition is that $\Omega(\tau = 0)$ contains domain Ω^{rot}, minimizer of (43), entirely. Naturally, Ω^{rot} is unknown. However, this constraint can easily be respected by choosing $\Omega(\tau = 0)$ equal to the entire image domain.

5 Segmentation of g-domains

Sections 3 and 4 deal with the segmentation of specific vector fields: translation fields and rotation fields, respectively. In this section, we extend the proposed method in order to define a general framework for the segmentation of vector fields of $\mathbb{R}^2$ that can be described by a finite number of parameters. As a result, we propose a step-by-step procedure from the definition of a vector field model (by means of a field line equation) to the segmentation algorithm.

5.1 Set of constraints and g-domain

A subset of $\mathbb{R}^n$, Δ, is called a set of constraints if it is equal to $\mathbb{R}^n$ or if it is given by the following set of intersections

$$\Delta = O \cap (\cap_{i=1}^{m} \Delta_i) \tag{51}$$

where O is a subset of $\mathbb{R}^n$ and Δ_i is defined by

$$\Delta_i = \{\alpha \in \mathbb{R}^n,\ \phi_i(\alpha) = 0\} \tag{52}$$

where each ϕ_i is a function C^1 from O to $\mathbb{R}$ and, for $j \neq i$, ϕ_i and ϕ_j are linearly independent.

A domain Ω of $\mathcal{F}$ is called a g-domain, where g is a smooth function from $\mathbb{R}^2 \times \mathbb{R}^n$ to $\mathbb{R}$, if and only if there exists a unique parameter $a(\Omega)$ of a set of constraints Δ such that for any field line L verifying $L \cap \Omega \neq \emptyset$ there exists a unique constant $c(L)$ of $\mathbb{R}$ such that

$$g(a(\Omega), x) = c(L),\ x \in L \cap \Omega\ . \tag{53}$$

Vector $a(\Omega)$ is called the g-parameter of Ω.

Translation domains and rotation domains are clearly two particular cases of g-domains with, respectively,

$$\left\{ \begin{array}{l} \Delta^{\mathrm{tra}} = \mathcal{C}^+ = O \cap \Delta_1 \\ g^{\mathrm{tra}}(a(\Omega), x) = a(\Omega) \cdot x \end{array} \right. , \tag{54}$$

where O is the set of x of $\mathbb{R}^2$ such that $x_1 \geq 0$ and $x_2 > -1$ and Δ_1 is defined by $\phi_1(\alpha) = |\alpha|^2 - 1$, and

$$\left\{ \begin{array}{l} \Delta^{\mathrm{rot}} = \mathbb{R}^2 \\ g^{\mathrm{rot}}(a(\Omega), x) = |x - a(\Omega)|^2 \end{array} \right. . \tag{55}$$

In our context, the specific value of $c(L)$ in (53) is of no importance and plays the role of an unnecessary parameter. Therefore, a condition equivalent to (53) while not involving $c(L)$ should be found. Let us parametrize L by p. For any $x(p)$ of $L \cap \Omega$

$$g(a(\Omega), x(p)) = c(L)\ . \tag{56}$$

The derivative of (56) with respect to p combined with (1) leads to the following system of equations

$$\left(\begin{array}{cc} \frac{\partial g}{\partial x_1}(a(\Omega), x(p)) & \frac{\partial g}{\partial x_2}(a(\Omega), x(p)) \\ E_2(x(p)) & -E_1(x(p)) \end{array} \right) \dot{x}(p) = M\ \dot{x}(p) \tag{57}$$

$$= 0\ . \tag{58}$$

Combining (2) and (58), it can be concluded that the determinant of M must be equal to zero. Therefore, a domain Ω of $\mathcal{F}$ is a g-domain if and only if there exists a unique $a(\Omega)$ of Δ such that for any x of Ω

$$\nabla_x g(a(\Omega), x) \cdot E(x) = 0 \tag{59}$$

where $\nabla_x g$ is the vector of components $\frac{\partial g}{\partial x_i}$.

5.2 Dominant g-parameter

From (59), it can be deduced that if Ω is a g-domain then $a(\Omega)$ is a global minimizer of

$$\begin{aligned} K^g_\Omega : \Delta &\to \mathbb{R} \\ \alpha &\mapsto \int_\Omega (\nabla_x g(\alpha, x) \cdot E(x))^2\ \mathrm{d}x\ . \end{aligned} \tag{60}$$

Indeed, K^g_Ω is clearly nonnegative and $K^g_\Omega(a(\Omega))$ is equal to zero.

Looking from a domain point of view (as opposed to the parameter point of view), it can also be deduced from (59) that Ω minimizes the following energy

$$\begin{aligned} G^g : \mathcal{F} &\to \mathbb{R} \\ \omega &\mapsto \int_\omega (\nabla_x g(a(\omega), x) \cdot E(x))^2 \, \mathrm{d}x \end{aligned} \tag{61}$$

with $a(\omega)$ defined as the unique global minimizer of K^g_ω.

However, there is no guarantee that for any ω of $\mathcal{F}$ there exists a unique global minimizer of K^g_ω and that K^g_ω is equal to zero for this minimizer. In other words, ω might not have a g-parameter (namely, if it is not a g-domain). Nevertheless, as long as K^g_ω has a unique global minimizer $\hat{a}(\omega)$, this minimizer is called the dominant g-parameter of ω.

5.3 Practical formulation

It is clear that any subdomain of a g-domain is a minimizer of energy (61). As a consequence, the problem of finding g-domains should be reformulated in finding g-domains having an area as big as possible. This is equivalent to minimizing $G^g(\Omega)$ while maximizing the area of Ω, *i.e.*, minimizing the following energy

$$\begin{aligned} J^g : \mathcal{F}^{\mathrm{g}} &\to \mathbb{R} \\ \Omega &\mapsto \int_\Omega (\nabla_x g(\hat{a}(\Omega), x) \cdot E(x))^2 \, \mathrm{d}x - \mu \int_\Omega \mathrm{d}x \end{aligned} \tag{62}$$

where $\mathcal{F}^{\mathrm{g}}$ is the set of domains of $\mathcal{F}$ having a dominant g-parameter, $\hat{a}(\Omega)$ is the dominant g-parameter of Ω, and μ is a positive constant.

5.4 Shape derivative

Following the methodology of Section 2.3, energy (62) is rewritten as a function of an evolution parameter τ

$$J^g(\tau) = \int_{\Omega(\tau)} (\nabla_x g(\hat{a}(\tau), x) \cdot E(x))^2 \, \mathrm{d}x - \mu \int_{\Omega(\tau)} \mathrm{d}x \tag{63}$$

where $\hat{a}(\tau)$ is a short notation for $\hat{a}(\Omega(\tau))$. Applying result (8) to each integral and following a development similar to the translation case (See Section 3.4), the shape derivative of (63) can be computed

$$\begin{aligned} \frac{\mathrm{d}J^g}{\mathrm{d}\tau}(\tau, V) = \frac{\mathrm{d}\hat{a}}{\mathrm{d}\tau}(\tau) \, \frac{\mathrm{d}K^g_{\Omega(\tau)}}{\mathrm{d}\alpha}|_{\hat{a}(\tau)} \\ - \int_{\partial\Omega(\tau)} \left[(\nabla_x g(\hat{a}(\tau), x(s)) \cdot E(s))^2 - \mu\right] \\ V(s) \cdot N_\tau(s) \, \mathrm{d}s \; . \end{aligned} \tag{64}$$

Expression (64) still contains a surface integral. As explained in Section 2.3, the shape derivative is readily usable if it contains only a line integral. Parameter $\hat{a}(\tau)$ minimizes $K^g_{\Omega(\tau)}$ on Δ (See Section 5.1). Therefore, there exists Lagrange multipliers λ^i_τ such that

$$\frac{\mathrm{d}K^g_{\Omega(\tau)}}{\mathrm{d}\alpha}|_{\hat{a}(\tau)} = \sum_{i=1}^{m} \lambda^i_\tau \, \frac{\mathrm{d}\phi_i}{\mathrm{d}\alpha}|_{\hat{a}(\tau)} \; . \tag{65}$$

Using (65) in (64) and following a development similar to the translation case (See Section 3.4), the final expression of the shape derivative of (63) is

$$\begin{aligned} \frac{\mathrm{d}J^g}{\mathrm{d}\tau}(\tau, V) = - \int_{\partial\Omega(\tau)} \left[(\nabla_x g(\hat{a}(\tau), x(s)) \cdot E(s))^2 - \mu\right] \\ V(s) \cdot N_\tau(s) \, \mathrm{d}s \; . \end{aligned} \tag{66}$$

5.5 Minimization algorithm

As presented in Section 2.3, the minimization of (62) can be achieved by iterating an active contour evolution equation deduced from shape derivative (66). The evolution equation is

$$\frac{\partial\Gamma}{\partial\tau}(\tau) = \left[(\nabla_x g(\hat{a}(\tau), x) \cdot E)^2 - \mu\right] \; N_\tau \tag{67}$$

where $\Gamma(\tau = 0)$ is an initial estimate of the segmentation contour. Dominant g-parameter $\hat{a}(\tau)$ of $\Omega(\tau)$ must be computed as the unique global minimizer of $K^g_{\Omega(\tau)}$ (See Section 5.2) in order to implement evolution (67).

6 Experiments

The proposed algorithm was applied to vector fields obtained in two ways: synthetic fields and dense optical flow fields.

6.1 Synthetic fields and optical flow

Synthetic fields are 100×100-pixel images composed of two regions. Each region can contain either a random field, a translation field, or a rotation field. These fields were obtained by assigning a two-dimensional vector with a norm equal to one to each pixel. The random field was obtained by drawing random numbers independently for each component and normalizing the resulting vector.

The optical flow fields between two consecutive frames of a video sequence was computed by a block matching technique similar to [22]. For each pixel of the first frame, a surrounding, centered block of 21×21 pixels was extracted and its best match in the second frame in terms of the zero-mean normalized sum of squared differences (ZNSSD) was found using a fast, suboptimal diamond search procedure [35]. In order to

limit the computation time to a reasonable value, the search procedure was restricted to a maximum amplitude of 4 pixels in the four directions. The vector of displacement from the original block to its matching block was assigned to the pixel at the center of the original block. In order to apply the proposed segmentation method, two processing steps were necessary. *(i)* Vectors equal to zero were replaced with vectors with random directions so that no global coherence was added to the field. *(ii)* The vectors were normalized.

6.2 Implementation

If the region, respectively object, of interest is assumed to be a translation domain, to have a motion of translation, evolution (30) should be implemented. Similarly, evolution (46) should be implemented if rotation is suspected. These active contour processes can be implemented with an implicit representation allowing changes of topology of the active contour such as level sets [4, 24, 10, 1, 16]. Since the vector fields used are assumed to contain only one object, changes of topology were not an issue. Therefore, we chose an explicit representation based on evolving spline curves [31, 6, 19, 25]. For translation, the segmentation algorithm can be described synthetically as follows

1. Choose weight μ of the area constraint
2. Choose an initial domain $\Omega(\tau = 0)$ according to Appendix C
3. Compute dominant translation parameter $\hat{a}(\tau)$ of $\Omega(\tau)$ as the solution of (35)
4. Compute energy (19) of $\Omega(\tau)$
5. For τ positive, if the energy of $\Omega(\tau)$ is equal to the energy of $\Omega(\tau - 1)$, then the algorithm has converged and $\Omega(\tau)$ is the solution of the segmentation, otherwise go to step 6
6. Update Ω according to a discretization of evolution (30)

$$\Gamma(\tau + 1) = \Gamma(\tau) + \alpha \ \left[(\hat{a}(\tau) \cdot E)^2 - \mu\right] \ N_\tau \quad (68)$$

where α is chosen heuristically in order to "ensure" stability of the evolution

$$\alpha = 1 \ / \ \max_{x \in \Gamma(\tau)} \left|(\hat{a}(\tau) \cdot E(x))^2 - \mu\right| \ . \quad (69)$$

7. Go back to step 3

The boundary Γ was represented by a spline passing through samples regularly spaced at a distance equivalent to 5 pixels. The discrete representation of Ω was the mask of pixels of Γ. Evolution (68) was applied to the samples of $\Gamma(\tau)$ and $\Gamma(\tau + 1)$ was computed as the spline passing through the moved samples. To maintain a distance of 5 pixels between the samples, periodic resampling was necessary.

Convergence was not tested exactly as stated in step 5, especially since the choice of α could cause endless oscillations around the solution. Instead, the algorithm was assumed to have converged when the energy was roughly constant during the last few iterations.

6.3 Translation domain

Since the background is not taken into account by the segmentation process, it was interesting to see the behavior of the algorithm when segmenting a translation domain on a translation background (See Figs. 2 and 3) and a rotation background (See Fig. 4). If the initial domain contains a reasonably higher portion of the object than the portion of the background, then the translation domain should be detected accurately (See Fig. 2). However, if the initial domain contains more background than object, then the notions of object and background naturally exchange for each other in the computation of the dominant translation parameter (See Fig. 3). In the three tests on synthetic translation domains (Figs. 2, 3, and 4), weight μ of the area constraint was taken equal to 0.1.

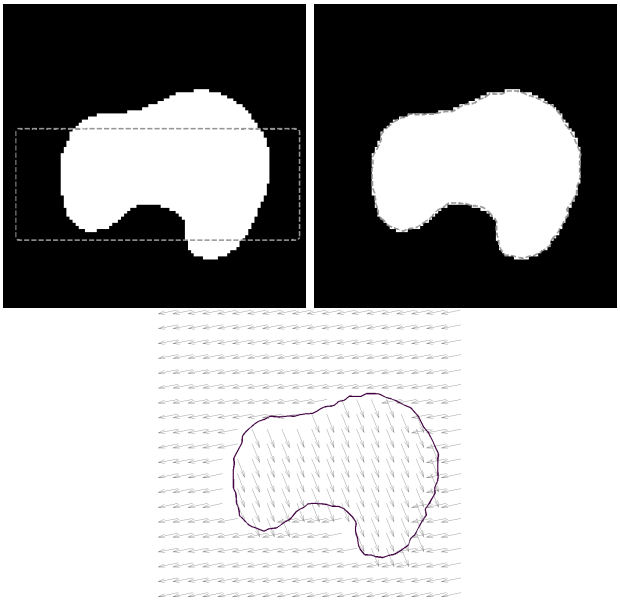

Figure 2: Segmentation of a translation domain on a translation background: *(from left to right and top to bottom)* the initial contour superimposed on the image of the first component of the vector field, the final contour on the same image, and the final contour on the vector field.

A real-world, standard, sport sequence was also used to test the proposed algorithm, as if part of a larger

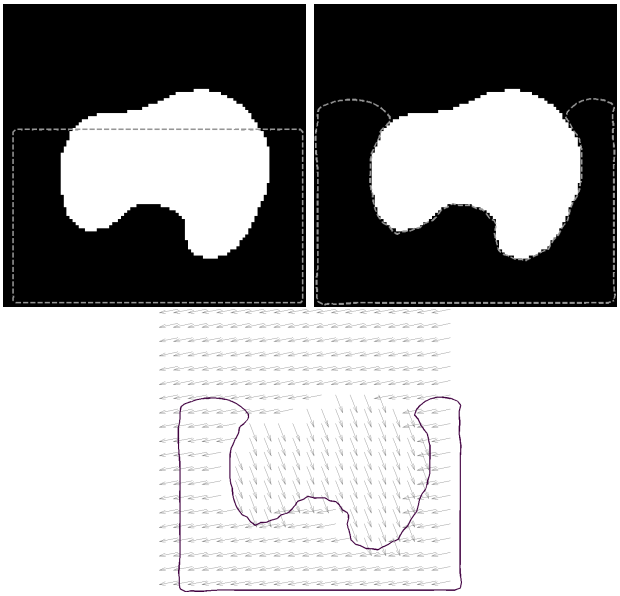

Figure 3: Segmentation (interrupted before convergence) of a translation domain on a translation background: *(from left to right and top to bottom)* the initial contour superimposed on the image of the first component of the vector field, the final contour on the same image, and the final contour on the vector field.

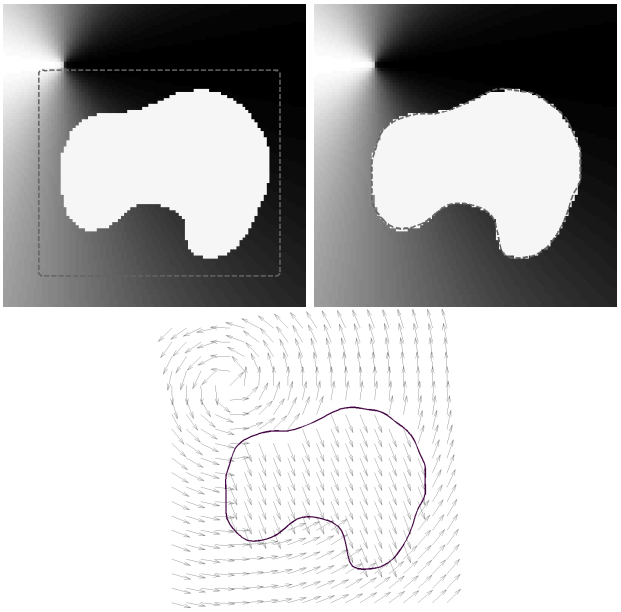

Figure 4: Segmentation of a translation domain on a rotation background: *(from left to right and top to bottom)* the initial contour superimposed on the image of the first component of the vector field, the final contour on the same image, and the final contour on the vector field.

processing chain. The optical flow between frames 15 and 16 of sequence "football" was computed as explained in Section 6.1. The sequence is in the CIF format: it is composed of 352×288-pixel frames. The main flow is due to the motion of the player in the center of the field of view. The segmentation of the optical flow is shown in Figs. 5 and 6. As far as the optical flow is concerned, the segmentation seems accurate (See Fig. 5 and the image on the left in Fig. 6). When superimposing the segmentation on frame 15 (See the image on the right in Fig. 6), the contour does not outline the player very precisely. Indeed, the optical flow is not accurate at the boundary of objects and in homogeneous or nearly homogeneous regions. It is a consequence of the block matching method when a block contains parts of different moving objects and when the correlation function is too flat and has several local minima, respectively. However, the purpose of this experiment was to test the proposed algorithm on a realistic optical flow, *i.e.* quite complex and noisy. In that respect, the result is satisfying. With sequence "football", weight μ of the area constraint was taken equal to 0.05, which is consistent with the value used with the synthetic vector fields while being a little smaller to account for noise. Indeed, a high value of μ increases the tolerance on the error of the segmentation term of evolution (30), implying a higher probability to include incorrect vectors in the segmentation.

6.4 Rotation domain

Similarly to the translation case, segmentation of a rotation domain was evaluated with several backgrounds: a translation background (See Figs. 7 and 8), a rotation background (See Fig. 9), and a random background (See Fig. 10). Two elements can be noticed on Figs. 7 and 8. First, since a rotation domain potentially contains vectors in all directions, there is an inevitable match with the direction of the translation in the background. Therefore, some vectors of the background close to the object and which happen to have a direction plausible in terms of the rotation might be

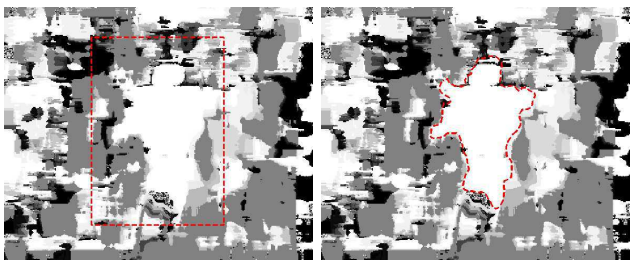

Figure 5: Segmentation of the optical flow of frame 15 of sequence "football": the initial contour superimposed on the image of the first component of the vector field *(left)* and the final contour on the same image *(right)*.

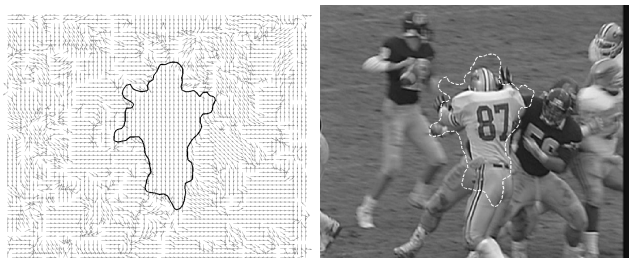

Figure 6: Segmentation of the optical flow of frame 15 of sequence "football" superimposed on the vector field *(left)* and superimposed on frame 15 *(right)*.

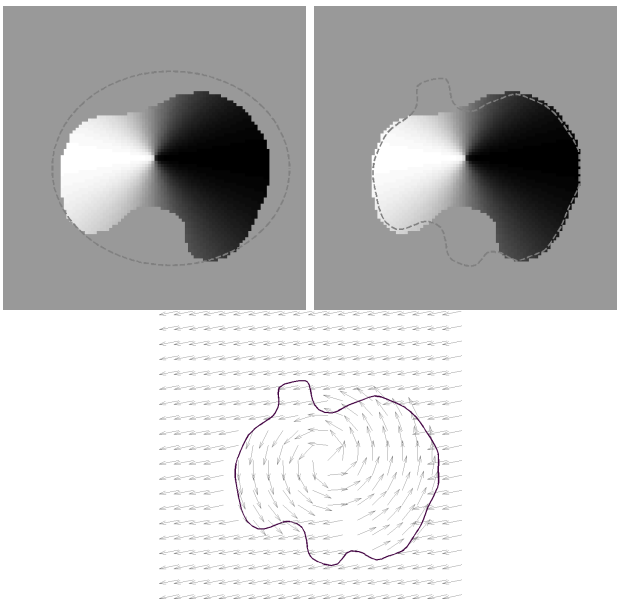

Figure 7: Segmentation of a rotation domain on a translation background: *(from left to right and top to bottom)* the initial contour superimposed on the image of the first component of the vector field, the final contour on the same image, and the final contour on the vector field.

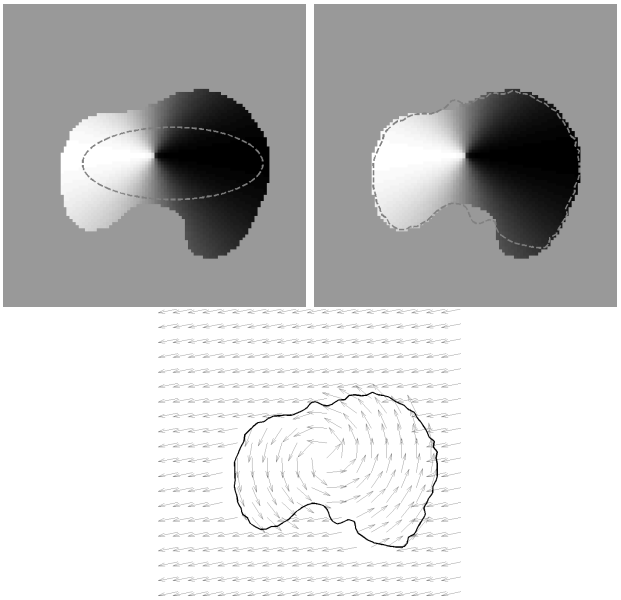

Figure 8: Segmentation of a rotation domain on a translation background: *(from left to right and top to bottom)* the initial contour superimposed on the image of the first component of the vector field, the final contour on the same image, and the final contour on the vector field.

included in the segmentation. Second, the segmentation is different whether the initial contour is inside or outside the object. Nevertheless, it has the same shape and behavior regarding translation vectors in the neighborhood of the object. This tends to show that, in this configuration of object and background vector fields, energy (43) is flat around the solution and has several local minima. With a rotation background having a rotation center far enough from the rotation center of the object, the segmentation is satisfying (See Fig. 9). Although an extensive study of the robustness and accuracy of the proposed method is out of the scope of this paper, it can be expected that segmentation becomes less accurate as the rotation centers of the background and the object get closer. The last experiment with a synthetic rotation domain was done with a random background. The segmentation shown in Fig. 10 seems accurate. In the four tests on synthetic rotation domains (Figs. 7, 8, 9 and 10), weight μ of the area constraint was taken equal to 10. This value, significantly higher than the values used for translation domains, tends to show that rotation energy (43) requires more tolerance on its segmentation term to segment the whole object than translation energy (19) does.

A real-world, somewhat artificial sequence was also used to test the proposed algorithm, as if part of a larger processing chain. A sponge was rotated manually by a few degrees around its center on a still background. A sequence composed of two 640×480-pixel frames was made and the optical flow between these frames was computed (See Fig. 11). The segmentation is shown in Fig. 12. Since the optical flow in the upper part of the background is mostly equal to zero, it was replaced with a random field as explained in Section 6.1. The lower part of the optical flow of the background was already randomly distributed. The segmentation of the optical flow, superimposed on the first frame of the sequence, appears to outline the sponge accurately.

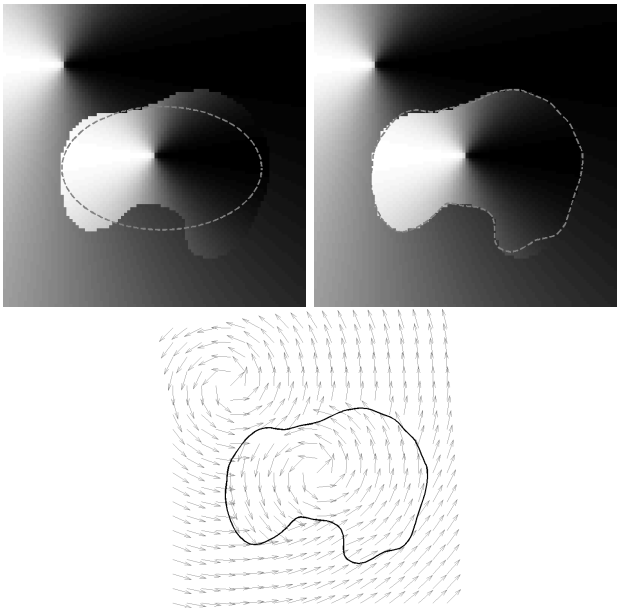

Figure 9: Segmentation of a rotation domain on a rotation background: *(from left to right and top to bottom)* the initial contour superimposed on the image of the first component of the vector field, the final contour on the same image, and the final contour on the vector field.

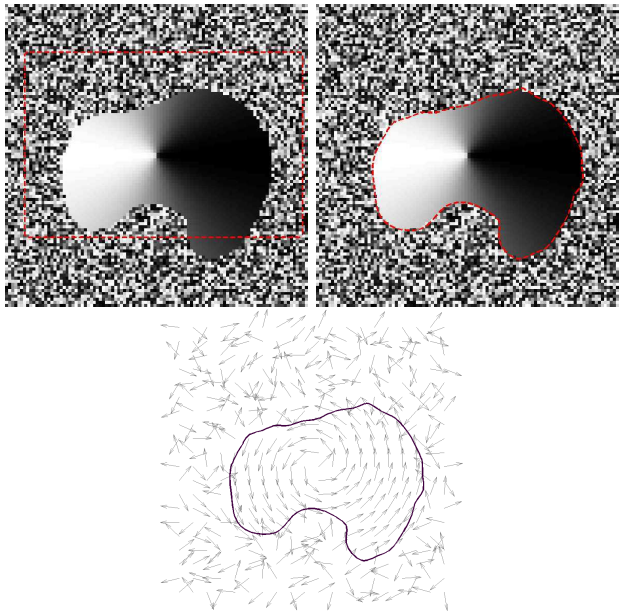

Figure 10: Segmentation of a rotation domain on a random background: *(from left to right and top to bottom)* the initial contour superimposed on the image of the first component of the vector field, the final contour on the same image, and the final contour on the vector field.

7 Conclusion

A methodology was proposed for the segmentation of vector fields of $\mathbb{R}^2$ that can be described by a finite number of parameters. The idea is to characterize a specific vector field by its underlying field lines. Given the type of subfield to be segmented (*e.g.*, translation or rotation), a specific model must be defined by means of the general form of the parametric equations of the field lines (straight lines or circles, respectively). The segmentation problem is expressed as the minimization with respect to the segmentation domain of an energy deduced from the field line equations. The minimization is rewritten into a shape optimization and solved by a spline-based active contour procedure requiring the choice of an initial estimate. The parameters of the field line equations are computed as part of the evolution process of the active contour (normal to the straight lines and center of the circles, respectively).

The method proved to work well for translation domains and rotation domains. Furthermore, it provides a general framework for more complex vector fields. However, it is adapted to normalized vector fields. Therefore, the necessary normalization step prior to the segmentation of an unnormalized field induces some loss of information: *(i)* A vector with a small norm and a random direction within a coherent region (a "noise" vector) will have, after normalization, as much influence on the computation of the dominant g-parameter as a vector with a large norm and a coherent direction; *(ii)* It is not possible to make the distinction between two translation domains having different norms but the same direction. As a consequence, further developments should use the "natural" vector field and take the norm of the vectors into account.

A Domain with no dominant translation parameter

Let Ω be a domain such that there exists a diffeomorphism t from $\mathbb{R}^2$ to $\mathbb{R}^2$ such that for any x of Ω

$$t(\Omega) = \Omega \tag{70}$$
$$|\det(J_t(x))| = 1 \tag{71}$$
$$E(t(x)) \cdot E(x) = 0 \tag{72}$$

where J_t is the Jacobian matrix of t. The orthogonality between $E(t(x))$ and $E(x)$ implies that

$$E_1(t(x)) = \epsilon\ E_2(x),\ \epsilon \in \{-1, 1\} \tag{73}$$
$$E_2(t(x)) = -\epsilon\ E_1(x) \tag{74}$$
$$E_1(t(x))\ E_2(t(x)) = -E_1(x)\ E_2(x)\ . \tag{75}$$

Matrix Q_Ω defined in (32) has the following form

$$Q_\Omega = \begin{pmatrix} a_1 & b \\ b & a_2 \end{pmatrix} \tag{76}$$

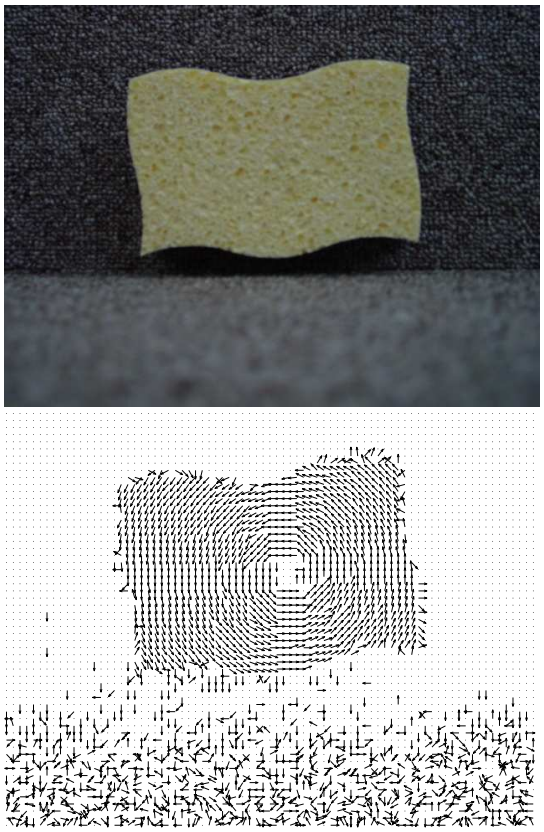

Figure 11: Rotating sponge on a still background: sponge before rotation *(top)* and optical flow of the rotation before processing as explained in Section 6.1 *(bottom)*.

where a_1, a_2, and b are equal to

$$a_i = \int_\Omega E_i(x)^2 \, \mathrm{d}x, \; i \in \{1, 2\} \tag{77}$$

$$b = \int_\Omega E_1(x) \; E_2(x) \, \mathrm{d}x \; . \tag{78}$$

We have

$$\begin{aligned} a_1 &= \int_\Omega E_2(t(x))^2 \, \mathrm{d}x && (79)\\ &= \int_{t(\Omega)} E_2(y)^2 \; |\det(J_t(y))| \, \mathrm{d}y && (80)\\ &= \int_{t(\Omega)} E_2(y)^2 \, \mathrm{d}y && (81)\\ &= \int_\Omega E_2(y)^2 \, \mathrm{d}y && (82)\\ &= a_2 \; . && (83) \end{aligned}$$

Moreover, we have

$$\begin{aligned} b &= -\int_\Omega E_1(t(x)) \; E_2(t(x)) \, \mathrm{d}x && (84)\\ &= -\int_{t(\Omega)} E_1(y) \; E_2(y) \; |\det(J_t(y))| \, \mathrm{d}y && (85)\\ &= -\int_{t(\Omega)} E_1(y) \; E_2(y) \, \mathrm{d}y && (86)\\ &= -\int_\Omega E_1(y) \; E_2(y) \, \mathrm{d}y && (87)\\ &= -b \; . && (88) \end{aligned}$$

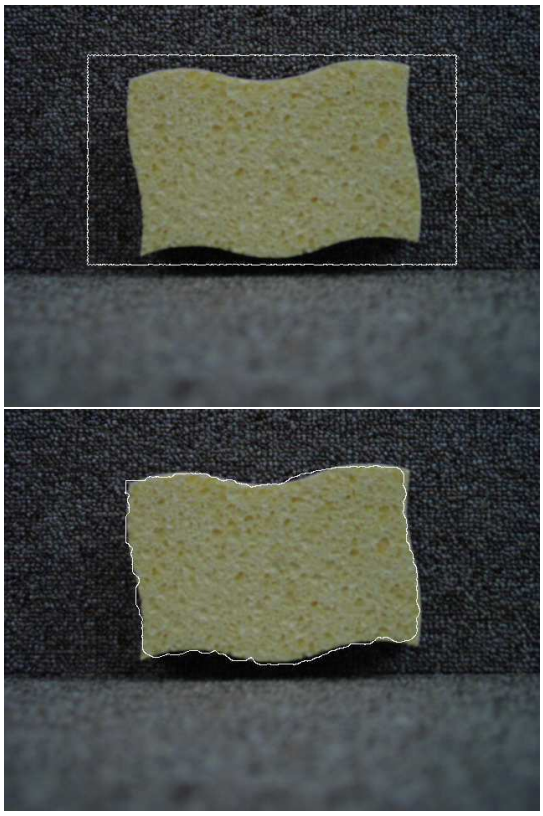

Figure 12: Segmentation of the optical flow superimposed on the image of the sponge before rotation (initialization *(top)* and solution *(bottom)*).

Therefore, b is equal to zero. In conclusion, Q_Ω is equal to the identity matrix times a constant. As shown in Section 3.5, this means that Ω has no dominant translation parameter.

For instance, a disk containing vectors rotating around the center of the disk has no dominant translation parameter. Indeed, it suffices to choose t as the rotation of $\frac{\pi}{2}$ around the center of the disk.

B Domain with no dominant rotation parameter

Taking the opposite of the equivalence of existence of a dominant rotation parameter proposed in Section 4.5, it can be stated that Ω has no dominant rotation pa-

rameter if and only if the determinant of Q_Ω is equal to zero. Explicitly, it means that

$$\int_\Omega E_1(x)^2 \, \mathrm{d}x \int_\Omega E_2(x)^2 \, \mathrm{d}x = \left(\int_\Omega E_1(x) \, E_2(x) \, \mathrm{d}x \right)^2 . \tag{89}$$

According to Cauchy-Schwarz, (89) is a superior-or-equal inequality in general. It is an equality, like in the present case, if and only if there exists a constant λ of $\mathbb{R}$ such that

$$E_2(x) = \lambda \, E_1(x) \tag{90}$$

for any x of Ω. However, E being normalized, for any x of Ω we also have

$$E_1(x)^2 + E_2(x)^2 = 1 . \tag{91}$$

From (90) and (91), it can easily be deduced that E is constant within Ω. In other words, Ω is a translation domain.

Since this result was obtained by a series of equivalences, it can be concluded that a domain has no dominant rotation parameter if and only if it is a translation domain.

C Initial segmentation of a translation domain

In Section 3.5, it is shown that a domain Ω has a dominant translation parameter if and only if there is no constant λ such that

$$Q_\Omega = \lambda \, Id \tag{92}$$

where Id is the identity matrix or, equivalently,

$$\int_\Omega E_1^2(x) \, \mathrm{d}x = \lambda \tag{93}$$

$$\int_\Omega E_2^2(x) \, \mathrm{d}x = \lambda \tag{94}$$

$$\int_\Omega E_1(x) \, E_2(x) \, \mathrm{d}x = 0 . \tag{95}$$

Vector field E being normalized, E_2^2 can be replaced with $1 - E_1^2$ in (94). As a result, (93) and (94) can be combined into

$$\int_\Omega E_1^2(x) \, \mathrm{d}x = \frac{|\Omega|}{2} \tag{96}$$

where $|\Omega|$ is the measure of Ω. Therefore, Ω has a dominant translation parameter if and only if

$$\int_\Omega E_1^2(x) \, \mathrm{d}x \neq \frac{|\Omega|}{2} \tag{97}$$

or

$$\int_\Omega E_1(x) \, E_2(x) \, \mathrm{d}x \neq 0 . \tag{98}$$

Let Ω^{tra} be the (unknown) minimizer of (19). It is assumed that

$$\Omega \supset \Omega^{\mathrm{tra}} \tag{99}$$

and

$$|\Omega / \Omega^{\mathrm{tra}}| < \frac{\sqrt{2}}{2} |\Omega^{\mathrm{tra}}| \tag{100}$$

where A/B is the intersection between A and the complement of B. Note that (100) is equivalent to

$$|\Omega| < (1 + \frac{\sqrt{2}}{2}) |\Omega^{\mathrm{tra}}| . \tag{101}$$

Our purpose is to show that if conditions (99) and (100) are respected, then (97) or (98) is true.

Since E is normalized, there exists θ, a function from $\mathbb{R}^2$ to $[0, 2\pi]$, such that

$$E(x) = \begin{pmatrix} \sin(\theta(x)) \\ \cos(\theta(x)) \end{pmatrix} . \tag{102}$$

Furthermore, Ω^{tra} being a translation domain, there exists a constant θ^{tra} such that for any x of Ω^{tra}

$$\theta(x) = \theta^{\mathrm{tra}} . \tag{103}$$

Finally, note that

$$\min_{\theta \in [0, 2\pi]} \{ \max \{ |\sin(2\theta)|, |\cos(2\theta)| \} \} = \frac{\sqrt{2}}{2} . \tag{104}$$

Combining (100) and (104), it can be deduced that

$$|\Omega / \Omega^{\mathrm{tra}}| < |\sin(2\theta^{\mathrm{tra}})| \, |\Omega^{tra}| \tag{105}$$

or

$$|\Omega / \Omega^{\mathrm{tra}}| < |\cos(2\theta^{\mathrm{tra}})| \, |\Omega^{tra}| . \tag{106}$$

• First case: Inequality (105) is true. We have

$$\left| \int_{\Omega / \Omega^{\mathrm{tra}}} E_1(x) \, E_2(x) \, \mathrm{d}x \right| \leq \int_{\Omega / \Omega^{\mathrm{tra}}} |E_1(x) \, E_2(x)| \, \mathrm{d}x \tag{107}$$

$$\leq \int_{\Omega / \Omega^{\mathrm{tra}}} \frac{|\sin(2\theta(x))|}{2} \, \mathrm{d}x \tag{108}$$

$$\leq \int_{\Omega / \Omega^{\mathrm{tra}}} \frac{1}{2} \, \mathrm{d}x \tag{109}$$

$$\leq \frac{1}{2} \, |\Omega / \Omega^{\mathrm{tra}}| \tag{110}$$

$$< \frac{1}{2} \, |\sin(2\theta^{\mathrm{tra}})| \, |\Omega^{\mathrm{tra}}| \tag{111}$$

It can be concluded that, in particular,

$$\int_{\Omega / \Omega^{\mathrm{tra}}} E_1(x) \, E_2(x) \, \mathrm{d}x \neq -\frac{1}{2} \, \sin(2\theta^{\mathrm{tra}}) \, |\Omega^{\mathrm{tra}}| . \tag{112}$$

Besides

$$\int_{\Omega} E_1(x)\ E_2(x)\ \mathrm{d}x = \int_{\Omega^{\mathrm{tra}}} E_1(x)\ E_2(x)\ \mathrm{d}x + \int_{\Omega/\Omega^{\mathrm{tra}}} E_1(x)\ E_2(x)\ \mathrm{d}x \tag{113}$$

$$= \frac{1}{2}\ \sin(2\theta^{\mathrm{tra}})\ |\Omega^{\mathrm{tra}}| + \int_{\Omega/\Omega^{\mathrm{tra}}} E_1(x)\ E_2(x)\ \mathrm{d}x\ . \tag{114}$$

Combining (112) and (114), it can be concluded that

$$\int_{\Omega} E_1(x)\ E_2(x)\ \mathrm{d}x \neq 0\ . \tag{115}$$

• Second case: Inequality (106) is true. We have

$$\left|\int_{\Omega/\Omega^{\mathrm{tra}}}\left(E_1(x)^2 - \frac{1}{2}\right)\ \mathrm{d}x\right| = \left|\int_{\Omega/\Omega^{\mathrm{tra}}} E_1(x)^2\ \mathrm{d}x - \frac{|\Omega/\Omega^{\mathrm{tra}}|}{2}\right| \tag{116}$$

$$\leq \int_{\Omega/\Omega^{\mathrm{tra}}}\left|E_1(x)^2 - \frac{1}{2}\right|\ \mathrm{d}x \tag{117}$$

$$\leq \int_{\Omega/\Omega^{\mathrm{tra}}}\left|\sin^2(\theta(x)) - \frac{1}{2}\right|\ \mathrm{d}x \tag{118}$$

$$\leq \int_{\Omega/\Omega^{\mathrm{tra}}} \frac{|\cos(2\theta(x))|}{2}\ \mathrm{d}x \tag{119}$$

$$\leq \int_{\Omega/\Omega^{\mathrm{tra}}} \frac{1}{2}\ \mathrm{d}x \tag{120}$$

$$\leq \frac{1}{2}\ |\Omega/\Omega^{\mathrm{tra}}| \tag{121}$$

$$< \frac{1}{2}\ |\cos(2\theta^{\mathrm{tra}})|\ |\Omega^{\mathrm{tra}}|\ . \tag{122}$$

It can be concluded that, in particular,

$$\int_{\Omega/\Omega^{\mathrm{tra}}} E_1(x)^2\ \mathrm{d}x - \frac{|\Omega/\Omega^{\mathrm{tra}}|}{2} \neq \frac{1}{2}\ \cos(2\theta^{\mathrm{tra}})\ |\Omega^{\mathrm{tra}}| \tag{123}$$

$$\iff \int_{\Omega/\Omega^{\mathrm{tra}}} E_1(x)^2\ \mathrm{d}x + (\sin^2(\theta^{\mathrm{tra}}) - \frac{1}{2})\ |\Omega^{\mathrm{tra}}| \neq \frac{|\Omega/\Omega^{\mathrm{tra}}|}{2} \tag{124}$$

$$\iff \int_{\Omega/\Omega^{\mathrm{tra}}} E_1(x)^2\ \mathrm{d}x + \int_{\Omega^{\mathrm{tra}}} E_1(x)^2\ \mathrm{d}x \neq \frac{|\Omega/\Omega^{\mathrm{tra}}|}{2} + \frac{|\Omega^{\mathrm{tra}}|}{2} \tag{125}$$

$$\iff \int_{\Omega} E_1(x)^2\ \mathrm{d}x \neq \frac{|\Omega|}{2}\ . \tag{126}$$

As a conclusion, if initial domain $\Omega(\tau)$ respects conditions (99) and (100), then it has a dominant translation parameter. Intuitively, evolution (30) will make $\Omega(\tau)$ shrink until, ideally,

$$\Omega(\tau = 0) = \Omega^{\mathrm{tra}}\ . \tag{127}$$

Therefore, conditions (99) and (100) should hold for all τ positive, until convergence.

D Initial segmentation of a rotation domain

The opposite of the equivalence of nonexistence of a dominant rotation parameter proposed in Appendix B reads that a domain has a dominant rotation parameter if and only if it is not a translation domain. Let Ω^{rot} be the (unknown) minimizer of (43). It is assumed that initial domain $\Omega(\tau = 0)$ is such that

$$\Omega(\tau = 0) \supset \Omega^{\mathrm{rot}}\ . \tag{128}$$

Clearly, since $\Omega(\tau = 0)$ contains a rotation domain, it cannot be a translation domain. Therefore, it can be concluded that it has a dominant rotation parameter. Intuitively, evolution (46) will make $\Omega(\tau)$ shrink until, ideally,

$$\Omega(\tau = 0) = \Omega^{\mathrm{rot}}\ . \tag{129}$$

Therefore, condition (128) should hold for all τ positive, until convergence.

References

[1] D. Adalsteinsson and J. A. Sethian. The fast construction of extension velocities in level set methods. *J. Comp. Phys.*, 148:2–22, 1999.

[2] G. Aubert, M. Barlaud, O. Faugeras, and S. Jehan-Besson. Image segmentation using active contours: Calculus of variations or shape gradients? *SIAM J. Appl. Math.*, 63:2128–2154, 2003.

[3] G. Aubert, R. Deriche, and P. Kornprobst. Computing optical flow via variational techniques. *SIAM J. Appl. Math.*, 60:156–182, 1999.

[4] G. Barles. Remarks on a flame propagation model. Technical Report 464, Team Sinus, INRIA, Sophia Antipolis, France, 1985.

[5] L. Blanc-Féraud, M. Barlaud, and T. Gaidon. Motion estimation involving discontinuities in a multiresolution scheme. *Optical Engineering*, 32:1475–1482, 1993.

[6] P. Brigger, J. Hoeg, and M. Unser. B-spline snakes: A flexible tool for parametric contour detection. *IEEE Trans. Imag. Proc.*, 9:1484–1496, 2000.

[7] V. Caselles, F. Catté, T. Coll, and F. Dibos. A geometric model for active contours. *Nümerische Mathematik*, 66:1–31, 1993.

[8] V. Caselles, R. Kimmel, and G. Sapiro. Geodesic active contours. *Int. J. Comp. Vision*, 22:61–79, 1997.

[9] J. G. Choi and S.-D. Kim. Multi-stage segmentation of optical flow field. *Signal Processing*, 54:109–118, 1996.

[10] D. L. Chopp. Computing minimal surfaces via level set curvature flow. *J. Comp. Phys.*, 106:77–91, 1993.

[11] J. Condell, B. Scotney, and P. Morrow. Adaptative grid refinement procedures for efficient optical flow computation. *Int. J. Comp. Vision*, 61:31–54, 2005.

[12] D. Cremers and C. Schnörr. Motion competition: Variational integration of motion segmentation and shape regularization. In *Pattern Recognition*, pages 472–480, Zürich, Switzerland, 2002.

[13] D. Cremers and C. Soatto. Motion competition: A variational approach to piecewise parametric motion segmentation. *Int. J. Comp. Vision*, 62:249–265, 2005.

[14] M. C. Delfour and J.-P. Zolesio. *Shapes and geometries: Analysis, differential calculus and optimization*. Advances in Design and control. Society for Industrial and Applied Mathematics, Philadelphia (PA), USA, 2001.

[15] A. Giachetti and V. Torre. Refinement of optical flow estimation and detection of motion edges. In *European Conference on Computer Vision*, pages 151–160, Cambridge, UK, 1996.

[16] J. Gomes and O. D. Faugeras. Reconciling distance functions and level sets. *Journal of Visual Communication and Image Representation*, 11:209–223, 2000.

[17] M. Hintermüller and W. Ring. A second order shape optimization approach for image segmentation. *SIAM J. Appl. Math.*, 64:442–467, 2003.

[18] B. K. P. Horn and B. G. Schunck. Detemining optical flow. *Artificial Intelligence*, 17:185–203, 1981.

[19] M. Jacob, T. Blu, and M. Unser. A unifying approach and interface for spline-based snakes. In *SPIE International Symposium on Medical Imaging: Image Processing*, pages 340–347, San Diego (CA), USA, 2001.

[20] S. Jehan-Besson, M. Barlaud, and G. Aubert. Dream^{2}s: Deformable regions driven by an Eulerian accurate minimization method for image and video segmentation. *Int. J. Comp. Vision*, 53:45–70, 2003.

[21] M. Kass, A. Witkin, and D. Terzopoulos. Snakes: Active contour models. *Int. J. Comp. Vision*, 1:321–332, 1988.

[22] B. Lucas and T. Kanade. An iterative image registration technique with an application to stereo vision. In *International Joint Conference on Artificial Intelligence*, pages 674–679, Vancouver, Canada, 1981.

[23] D. Mumford and J. Shah. Optimal approximations by piecewise smooth functions and associated variational problems. *Comm. Pure Appl. Math.*, 42:577–685, 1989.

[24] S. Osher and J. A. Sethian. Fronts propagating with curvature-dependent speed: Algorithms based on Hamilton-Jacobi formulations. *J. Comp. Phys.*, 79:12–49, 1988.

[25] F. Precioso, M. Barlaud, T. Blu, and M. Unser. Smoothing B-spline active contour for fast and robust image and video segmentation. In *International Conference on Image Processing*, pages 137–140, Barcelona, Spain, 2003.

[26] R. Ronfard. Region-based strategies for active contour models. *Int. J. Comp. Vis.*, 13:229–251, 1994.

[27] T. Roy, M. Barlaud, E. Debreuve, and G. Aubert. Vector field segmentation using active contours: Regions of vectors with the same direction. In *Workshop on Variational, Geometric and Level Set Methods in Computer Vision*, Nice, France, 2003.

[28] O. Sanchez and F. Dibos. Displacement following of hidden objects in a video sequence. *Int. J. Comp. Vision*, 57:91–105, 2004.

[29] G. Sapiro. Vector (self) snakes: A geometric framework for color, texture and multiscale image

segmentation. In *International Conference on Image Processing*, pages 817–820, Lausanne, Switzerland, 1996.

[30] C. Schnörr. Computation of discontinuous optical flow by domain decomposition and shape optimization. *Int. J. Comp. Vision*, 8:153–165, 1992.

[31] M. Unser, A. Aldroubi, and M. Eden. B-spline signal processing: Part I - Theory. *IEEE Trans. Signal Proc.*, 41:821–833, 1993.

[32] J. Y. A. Wang and E. H. Adelson. Spatio-temporal segmentation of video data. In *SPIE on Image and Video Processing II*, volume 2182, pages 120–131, San Jose (CA), USA, 1994.

[33] J. Weickert and C. Schnörr. Variational optic flow computation with a spatio-temporal smoothness constraint. *Journal of Mathematical Imaging and Vision*, 14:245–255, 2001.

[34] S. F. Wu and J. Kittler. A gradient-based method for general motion estimation and segmentation. *Journal of Visual Communication and Image Representation*, 4:25–38, 1993.

[35] S. Zhu and K.-K. Ma. A new diamond search algorithm for fast block matching motion estimation. *IEEE Trans. Imag. Proc.*, 9:287–290, 2000.